ACS APPLIED MATERIALS & INTERFACES

RESEARCH ARTICLE

www.acsami.org

In vitro Studies and Preliminary In vivo Evaluation of Silicified Concentrated Collagen Hydrogels

Martín F. Desimone,[†,‡] Christophe Hélary,[†] Sandrine Quignard,[†] Ivo B. Rietveld,[§] Isabelle Bataille,[⊥,#] Guillermo J. Copello,[‡] Gervaise Mosser,[†] Marie-Madeleine Giraud-Guille,[†] Jacques Livage,[†] Anne Meddahi-Pellé,[⊥,#] and Thibaud Coradin*[,†]

[†]UPMC Univ Paris 06; CNRS, Chimie de la Matière Condensée de Paris, Collège de France, 11 place Marcelin Berthelot, F-75005 Paris, France

[‡]IQUIMEFA-CONICET, Facultad de Farmacia y Bioquimica, Universidad de Buenos Aires, 1113 Buenos Aires, Argentina

[§]Université Paris Descartes, Faculté de Pharmacie, Chimie Physique - Case 23, F-75006 Paris, France

[⊥]Institut National de le Santé et de la Recherche Médicale (INSERM), U698, CHU Xavier Bichat, Bât. Inserm, 46 rue Henri-Huchard, F-75018 Paris, France

[#]Université de Versailles Saint-Quentin-en-Yvelines, UFR Médicale Paris Ile de France Ouest, F-78280 Guyancourt, France

ABSTRACT: Hybrid and nanocomposite silica−collagen materials derived from concentrated collagen hydrogels were evaluated in vitro and in vivo to establish their potentialities for biological dressings. Silicification significantly improved the mechanical and thermal stability of the collagen network within the hybrid systems. Nanocomposites were found to favor the metabolic activity of immobilized human dermal fibroblasts while decreasing the hydrogel contraction. Cell adhesion experiments suggested that in vitro cell behavior was dictated by mechanical properties and surface structure of the scaffold. First-to-date in vivo implantation of bulk hydrogels in subcutaneous sites of rats was performed over the vascular inflammatory period. These materials were colonized and vascularized without inducing strong inflammatory response. These data raise reasonable hope for the future application of silica−collagen biomaterials as biological dressings.

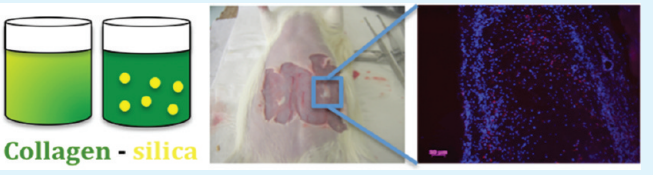

KEYWORDS: collagen, silica, hybrid materials, nanocomposites, biomaterials, subcutaneous implantation, vascular-inflammatory period

INTRODUCTION

Cell encapsulation technology finds exciting applications in medicine.[1,2] In the field of skin tissue engineering, one of the main challenges is to design cellularized devices that can promote tissue regeneration and/or wound healing.[3] Transplantation of dermal substitutes colonized by fibroblasts has shown several advantages over acellularized materials,[4] including controlled and continuous production of extracellular macromolecules and cytokines by dermal fibroblasts that favors neovascularization, cell proliferation and differentiation. Another advantage of cellularized materials is that they shorten the in vivo colonization time.[5]

Cellularized collagen hydrogels are commonly obtained using the method developed by Bell et al. consisting of neutralization of diluted (0.7 mg mL^{-1}) acid soluble collagen solutions extemporary prior to fibroblast encapsulation.[6] One of the main limitations of using those types of collagen gels as biomedical materials is related to their poor mechanical properties. In this case, fibroblasts easily contract the collagen network to a great extent. The cells within the contracted collagen gels exhibit phenotypic modifications and apoptosis, leading to the biological failure of the implant.[7−9]

Among different approaches to overcome this drawback, it has recently been demonstrated that concentrated collagen hydrogels can be considered as new candidates for dermal substitution because they are easy to handle, do not contract drastically, show improved fibroblast growth, and can be quickly integrated in vivo.[10] In the context of bone substitutes, mineralized collagen gels demonstrated to be a useful alternative to improve the mechanical properties of collagen gels.[11−14] Recently, we developed silica−collagen systems, either as hybrid hydrogels from aqueous silicate precursors[15] or as nanocomposite materials by addition of silica nanoparticles,[16] that are both compatible with simultaneous immobilization of fibroblasts.

To evaluate the potentialities of such silica−collagen systems as biomaterials, it was important to perform a first in vivo evaluation. Indeed, biomaterial surface properties play an important role in modulating cellular wound healing events. Foreign body reaction at the tissue/material may impact the biocompatibility of implanted biomaterial and tissue response. It is also crucial that the implanted systems are colonized by fibroblast cells, favoring neo-collagen formation, and by endothelial cells, allowing vascularization. In fact, although several examples of

Received: March 22, 2011
Accepted: September 12, 2011
Published: September 12, 2011

Scheme 1. Overview of the Preparation of Pure Collagen Hydrogels (Ch), Collagen−Colloidal Silica Nanocomposites (Nc), and Collagen−Silicate Hybrid Materials (Hy)

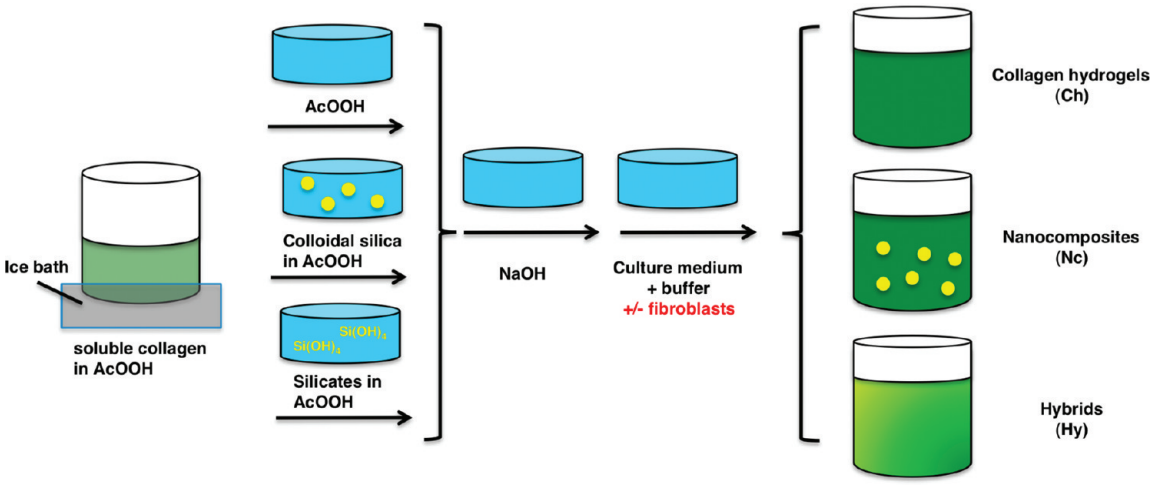

in vivo data of silica-based xerogels,[17] capsules,[18] and particles[19−21] have been reported, no data are, to the best of our knowledge, available about composite or hybrid hydrogels after subcutaneous implantation.

As a first step, we have investigated the tissue response of silica-collagen materials after one-week subcutaneous implantation in rat model. This period corresponds to the vascular-inflammatory step that is a critical to discriminate between potential candidates before undertaking longer and more extensive in vivo studies. In these conditions, we show here that suitable in vivo responses, i.e., fibroblast colonization and vascularization of the implant without inflammatory response, can be observed provided that higher collagen concentrations are used. We also demonstrate that these materials are compatible with fibroblast encapsulation while ensuring low contraction in vitro. All these data suggest that silica−collagen materials can be considered as potential candidates for biological dressings[22] that should now be further evaluated in terms of long-term degradation as well as regarding pharmacokinetics studies of the fate of silica in the human body.

EXPERIMENTAL SECTION

Silica−Collagen Materials Preparation and Characterization. Collagen type I was purified from rat tails and the concentration was estimated by hydroxyproline titration.[23] Silica nanoparticles 12 nm in size (Si12) (Ludox HS-40) and sodium silicate were purchased from Aldrich. Silica−collagen materials were prepared by mixing collagen solution with either silica molecular precursor (silicates),[15] leading to the simultaneous condensation of silica and collagen self-assembly (hybrid materials) or colloidal silica,[16] leading to their dispersion in the proteinaceous matrix (composite materials) (Scheme 1). Nanocomposites (Nc) were prepared by mixing 0.6 mL of a solution containing 2.8 mg mL^{-1} (Nc0, final concentration 0.8 mg mL^{-1}) or 10 mg mL^{-1} (Nc3, final concentration 3 mg mL^{-1}) collagen in 17 mM acetic acid with 0.8 mL of complete fibroblast culture medium in an ice bath. In parallel, a suspension of nanoparticles was acidified to pH 3.0 with acetic acid and added to the collagen solution in order to obtain a 10 mM final concentrations in the gel. The solution was then neutralized with 0.08 mL of 0.1 M NaOH, and finally 0.6 mL of a complete medium supplemented with fetal bovine serum (FBS) was added (Scheme 1). Hybrid materials (Hy0 and Hy3) were obtained using a similar protocol except for the use of a sodium silicate solution instead of a particle suspension. The reference collagen hydrogels (Ch0 and Ch3) were prepared following the same protocol previously described by Bell[6] and Hélary,[10] respectively.

Shear oscillatory measurements on samples were performed on a Bohlin Gemini rheometer (Malvern) equipped with plane acrylic 40 mm diameter geometry. Both base and geometry surfaces were rough in order to avoid sample slipping during measurements. All tests were performed at 37 °C. Mechanical spectra, i.e., storage, G', and loss, G'', modulus vs frequency, were recorded at an imposed 1% strain, which corresponded to nondestructive conditions (i.e., linear viscoelastic regime), as previously checked (data not shown).[10] To test all materials under the same conditions, before each run, the gap between base and geometry was chosen so that a slight positive normal force was applied to the gels during measurements. Four samples of each type were tested at day 1.

Differential scanning calorimetry (DSC) experiments were performed using a Mettler-Toledo (Switzerland) 822e thermal analyzer equipped with a Huber (Germany) TC100 cooling device. Indium (T_{fus} = 156.60 °C, ΔH_{fus} = 3267 J mol^{-1}) and zinc (T_{fus} = 419.53 °C, ΔH_{fus} = 7320 J mol^{-1}) were used for calibration of temperature and heat exchange. The initial samples were concentrated by removing about 50% of the water content. They were introduced into standard Mettler-Toledo 40 μL aluminum capsules and weighed on a microbalance sensitive to 0.01 mg.

The release of silica from the composite gels was investigated by Si titration using inductively coupled plasma atomic emission spectroscopy (ICP-AES) on the gel supernatant.[15,16] The determinations were performed at 251.6 nm using a PerkinElmer Analyst 100 apparatus with a slit of 0.2 nm and a flame of nitrous oxide-acetylene.

2D In vitro Experiments. Normal human dermal fibroblasts (Promocell) were grown in a complete medium and kept at 37 °C in a 95% air and 5% CO_2 atmosphere. Before confluence, fibroblasts were removed from culture flasks by treatment with 0.1% trypsin and 0.02% EDTA. Fibroblasts were used at passage 7 for all experiments.

To test cell adhesion on the different materials, we added 1×10^5 fibroblast cells at the surface of each gel. At 3, 6, and 24 h after cell seeding, the gels were rinsed three times with PBS and fixed with 4% paraformaldehyde for 1 h. Samples were again washed three times with PBS. Cells were permeabilized by Triton X-100 (0.05% in PBS-1% bovine serum albumin) for 10 min and the nuclei were stained with 4′,6′-diamidino-2-phénylindole (DAPI) (5 μg mL^{-1} in PBS) for 2 min. A count of remaining adherent cells was performed with a fluorescent

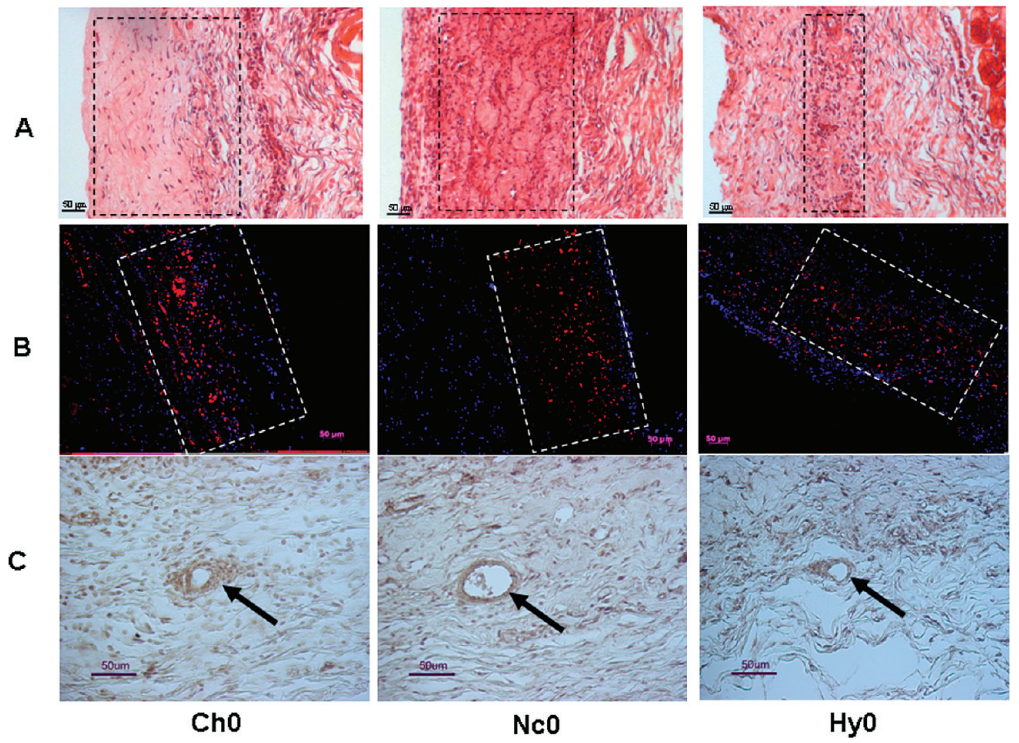

Figure 1. Histological and immunohistological studies 8 days postsurgery. Pure collagen (Ch0), nanocomposite (Nc0), and hybride (Hy0) scaffolds were implanted subcutanously. Sections were stained with hematoxylin-eosin (line A), detection of macrophages (CD68 marker) (line B), and endothelial cells (RECA-1 marker) (line C).

microscope, over a total of 7 random fields (×10 magnification) for each sample. Samples were run in triplicates.

The proliferation of adherent cells was determined by the tetrazolium assay.[24] This colorimetric assay is based on the ability of the mitochondrial dehydrogenase enzymes of living cells to convert 3-(4,5-dimethylthiazol-2-yl)-2,5-diphenyl-tetrazolium bromide (MTT) into an insoluble formazan. The medium was removed after 24 h, 7 and 21 days and a 5 mg/mL solution of MTT in PBS was added to the gels and incubated at 37 °C in a humidified 5% CO_2 air atmosphere for 4 h. Afterward, MTT solution was removed, the gels were washed three times with water and DMSO was added for 30 min. The optical density was recorded at 570 nm. Readings were converted to cell number using a standard curve. For each condition, sample number was three or more.

Samples for scanning electron microscopy (SEM) were fixed using 3.63% glutaraldehyde in 0.05 M sodium cacodylate buffer (pH 7.4) with 0.3 M saccharose for 1 h at 4 °C. Following fixation, samples were washed three times in the same buffer and then dehydrated in a graded series of ethanol (70%, 95% and two changes of alcohol 100%). Finally, the samples were subjected to supercritical drying and were gold sputter-coated for analysis using a Jeol JSM 5510LV SEM operating at 10 kV.

3D In vitro Experiments. For cell encapsulation, the same protocol described above for material preparation was used except for the addition of 0.6 mL of 1×10^5 fibroblast cells at the last step of the process (scheme 1). The cellular viability of entrapped cells was determined by the tetrazolium assay (MTT, described above). Cell-mediated gel contraction was evaluated by measuring the diameter of the samples every 7 days for 21 days.

In vivo Implantation. Both the procedure and the animal treatment complied with the Principles of Laboratory Animal Care formulated by the National Society for Medical Research. The studies were carried out under authorization no. 006235 of the Ministère de l'Agriculture, France. Nine adult Wistar male rats weighing 250 g (Wi/Wi, Charles-Rivers France) were anaesthetized by intraperitoneal injection of sodium pentobarbital solution (30 mg/kg, Centravet France). The abdomen was shaved and disinfected. A vertical incision was made on the abdominal midline, and the 1 cm^2 samples were implanted in subcutaneous pocket ($n = 3$). The skin and the muscle layer were then sutured (Vicryl 4/0). After 8 days post surgery, the rats were euthanized by intraperitoneal injection of sodium pentobarbital (60 mg/kg). The gels were then sampled and fixed in 4% paraformaldehyde (Merck France) in PBS for 24 h, dehydrated and embedded in paraffin ($n = 3$).

Thick sections of 7 μm were performed[25] and stained with eosin-hemalun. Endothelial and macrophage cells were immunodetected by using RECA-1 primary antibody (1/10 dilution in blocking solution) and anti CD68 primary antibody (1/1000 v/v) (Euromedex, France), resepctively and incubated for 90 min in moist chamber with a secondary antibody (antimouse IgG biotin conjugated (DAKO) for RECA-1 and antimouse coupled with Rhodamine (Molecular Probe) for CD68 detection). Then, for RECA-1, endogenous peroxidases were inhibited by incubation at 37 °C with 3% H_2O_2. After washing, the samples were incubated for 45 min with streptavidin/peroxydase complex from DAKO diluted 1/300 in PBS 3% NaCl. After three rinses in PBS 3% NaCl, Peroxydase labeling was revealed for 15 min in a dark chamber using 3,3′-diaminobenzindine tetrahydrochloride (Sigma) in Tris-HCl, pH 7.6 and observed with Nikon E600 POL microscope. For CD68 detection, sections were incubated for 10 min in a DAPI bath (dilution: 1/50 000 v/v). To exclude nonspecific binding, controls were performed by omitting primary antibodies or by using irrelevant secondary antibodies. Finally, slides were rinsed three times in PBS and observed with a fluorescence microscope AXIO 100 (Zeiss).

RESULTS AND DISCUSSION

In vivo Evaluation of Nanocomposite and Hybrid Materials at Low Collagen Content. The first objective of this work was to evaluate the in vivo response of previously reported

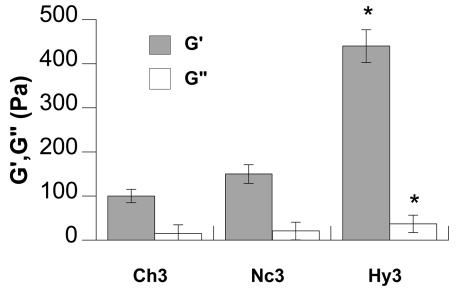

Figure 2. Storage (G') and loss (G'') moduli of the concentrated-collagen hydrogels (Ch3), nanocomposites (Nc3), and hybrids (Hy3). Results are expressed as mean ± SD from triplicates experiments. * indicates statistical significance ($p < 0.05$) from student test.

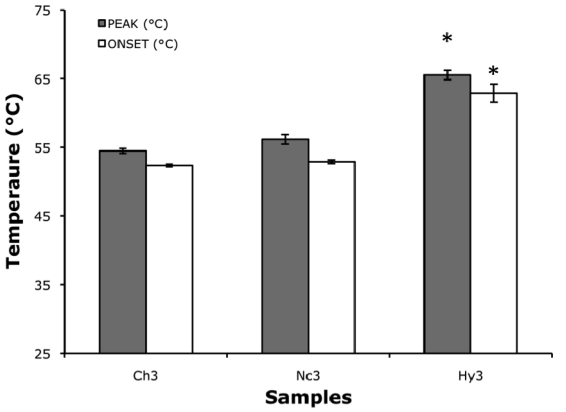

Figure 3. Denaturation temperature as characterized by onset and peak maximum of DSC signals for the concentrated-collagen hydrogels (Ch3), nanocomposites (Nc3), and hybrids (Hy3). Results are expressed as mean ± SD from triplicates experiments. * indicates statistical significance ($p < 0.05$) from student test.

silica-collagen nanocomposite and hybrid materials prepared at low collagen concentration (0.8 mg.ml^{-1}).[15,16] Eight days after the subcutaneous implantation within rat abdomen, histological analysis revealed a complete colonization of Ch0 and silicified collagen gels (Nc0 and Hy0) by the host cells (Figure 1A). The CD68 immunolabeling (red fluorescence) showed the presence of inflammatory cells within the low-concentrated collagen hydrogels (Figure 1B). The amount of macrophages seems to be slightly lower in Nc0 compared to Hy0 gels. Moreover, endothelial cells were detected by RECA-1 (brown staining) within these gels and in some cases organized cells in open tubular structures were observed (Figure 1C). Therefore, such a low collagen concentration leads to a very fast colonization of the materials by fibroblasts and endothelial cells. Whereas this situation indicates that the materials constitute a suitable environment for cell activity, the kinetics of the process are not compatible with a sustainable implant where scaffold degradation and neo-tissue formation should occur at a similar pace. In addition, the observed inflammatory response over this period shows unsuitable biocompatibility. These results are in good agreement with previous reports showing that low concentrated collagen gels are easily degraded both in vitro and in vivo.[10,26]

Preparation and Characterization of Concentrated Nanocomposite and Hybrid Materials. To overcome this problem, and based on the literature,[27,28] we hypothesized that an increase in collagen concentration would decrease the colonization rate and the inflammatory response. We therefore prepared hybrid and nanocomposite materials with a final collagen concentration of 3 mg mL^{-1}. Despite a significant increase in the viscosity of the starting collagen solution and silica concentration,[29,30] it was possible to add soluble silicate species and silica nanoparticles and to obtain homogeneous materials.

The mechanical properties of the silicified materials, Nc3 and Hy3, were investigated by rheological measurements and compared to the pure collagen hydrogel Ch3. Storage (G') and loss (G'') moduli were measured versus frequency. In all materials G' was at least ten times higher than G'', which is mainly related to a characteristic elastic behavior of collagen gels. As shown in Figure 2, both moduli G' and G'' increased in silicified collagen gels. The elastic modulus (G') was 1.5 and 4.5 times higher in Nc3 and Hy3 materials, respectively, reaching 450 Pa for the latter. In Nc3 gels, this increase is likely due to the role of silica nanoparticles as mineral charge for the collagen network, as often observed in nanocomposite materials. Hy3 materials prepared using a cogelation process exhibit even higher storage and loss moduli than Nc3. In addition, it is worth mentioning that these hybrids also have the brittle characteristics of sol−gel materials upon handling. These observations are in good agreement with previous reports on biopolymer−silica hybrid materials describing that the in situ condensation of silica molecular precursor leads to an interpenetrated network of bio-organic and mineral phases whose improved mechanical stability is due to both the hardness of silica and the interactions at the biomineral surface.[12,31,32] Although direct comparison with other hydrogels is rendered difficult by the wide range of compositions and cross-linking strategies found in the literature, it is interesting to note that here-described materials exhibiting storage moduli in the 100−500 Pa range are of similar mechanical stability as described derivatives of a very popular synthetic polymer used in biomaterial science, poly-N-isopropylacrylamide (p-NIPAM) gels.[33,34]

In parallel, the thermal stability of collagen was studied by DSC. The peak temperature of collagen denaturation was 55 °C for pure collagen and did not change significantly in the presence of silica nanoparticles. On the other hand, in Hy3 hybrid materials a significant increase in collagen thermal stability was observed. Indeed, the peak temperature of collagen denaturation was 65 °C, which is 10 °C higher than Ch3 gels (Figure 3). This can be related to a "confinement process", wherein the protein is restricted in its ability to undergo conformational changes. In that hypothesis, the silicates may cover the collagen fibrils, limiting protein unfolding possibility and therefore increasing denaturation temperature, as already observed for many silica-entrapped enzymes.[35] Such an increase was already observed for diluted collagen gels but with a maximum variation of 4 °C.[16] Here a considerable higher thermal stability (up to 10 °C) is obtained because of the higher collagen concentration. Indeed, the body temperature is not expected to go beyond ca. 40 °C, but these thermal effects constitute a clear indication of the overall benefit of silicification on collagen stability.

2D Culture of Fibroblasts on Concentrated Silica−Collagen Materials. In a first step, the suitability of the silicified materials to promote cell adhesion and proliferation on their surface was studied. As shown in Figure 4a, the cell density did not significantly evolve during 24 h culture neither on Ch3 nor on Nc3, suggesting that cell adhesion occurs rapidly but do not promote cell division. For Hy3, the initial (i.e., after 3 h seeding) cell density is similar to the two other hydrogels but it increases

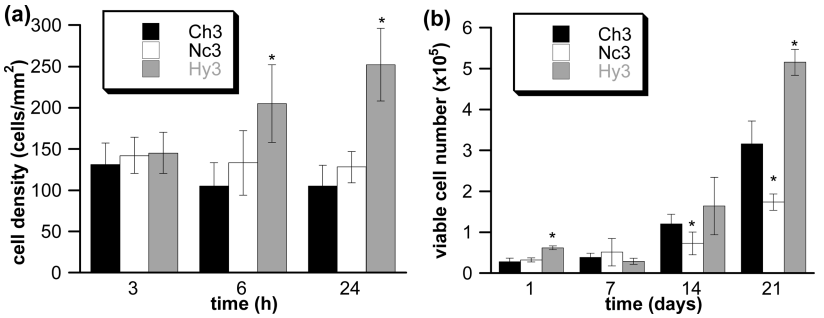

Figure 4. (a) Fibroblast adhesion and (b) proliferation as a function of time for collagen hydrogels (Ch3), nanocomposites (Nc3), and hybrids (Hy3). Results are expressed as mean ± SD from triplicates experiments. * indicates statistical significance ($p < 0.05$) from student test.

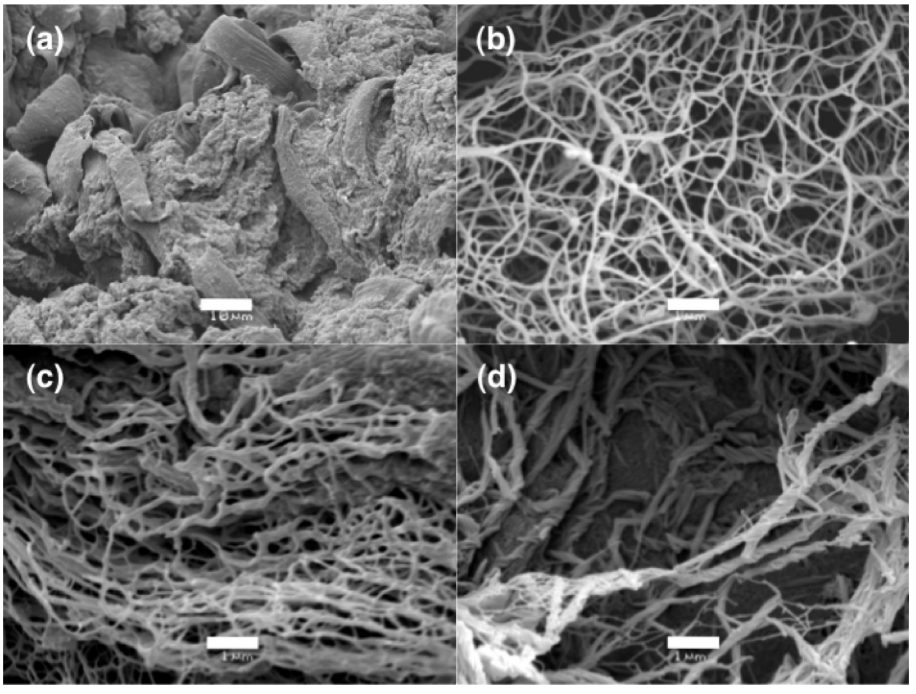

Figure 5. SEM images of (a) fibroblast cells colonizing Ch3 hydrogels (scale bar = 10 μm) and collagen organization in (b) Ch3, (c) Nc3, and (d) Hy3 hydrogels (scale bar = 1 μm) after 21 days of 2D cell culture.

after 6 h and remains significantly larger than the control, suggesting that fibroblasts could efficiently anchor on the surface and start to proliferate. This better affinity of cells for the hybrid surface was confirmed when proliferation assays were performed over a 3-week period (Figure 4b). Noticeably, the pure collagen hydrogel also favors cell proliferation over this period but the final cell number was lower than for Hy3 because of the lowest cell density at 24 h. Nc3 also allowed cell proliferation but to a much lower extent than Ch3 and Hy3.

The hydrogel surface was also imaged by SEM at the end of the culture period (Figure 5). As seen in Figure 5a for Ch3, a high density of fibroblast cells are easily visualized on the hydrogels surface, some of them penetrating the hydrogel, in agreement with reported colonization of these materials. At higher magnification, it is possible to observe the collagen network whose morphology highly depends on the considered materials. For Ch3, it consists of thin fibrils interconnected to form a highly porous network (Figure 5b). For Nc3, the fibrils are much thicker and pore size decreases but the interconnected network is well-preserved (Figure 5c). In the case of Hy3, the formation of large fibrillar ropes and large pores are observed (Figure 5d) These morphologies are in good agreement with previous data obtained for diluted collagen hydrogels, reflecting the influence of silica colloids, which favor fibril aggregation and lead to larger fibers, and silica polymers, which coat individual fibrils and interfere with their aggregation, on collagen fibril organization.[15,16]

The adhesion/proliferation of cells on a substrate depends on both the surface chemistry, i.e., the possibility for proteins involved in cell-binding phenomena such as integrins to be adsorbed, the macroporosity, and the mechanical stability of the hydrogel.[36−38] Here, we found that the hybrid system is the most efficient in favoring adhesion, although the collagen organization is strongly impact by the silicification process, suggesting that the increase in storage modulus is the key factor involved in this improvement. In contrast, the composite material shows no variation in adhesion compared to the control, in agreement with only minor improvement of its mechanical stability. In terms of proliferation, they are comparable for Ch3

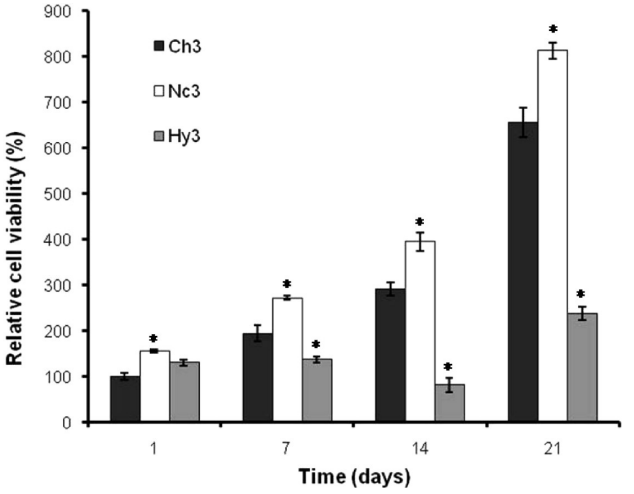

Figure 6. Relative metabolic activity of entrapped fibroblasts (MTT assay) compared to control collagen hydrogels at day 1. Results are expressed as mean ± SD from triplicates experiments. * indicates statistical significance ($p < 0.05$) from student test.

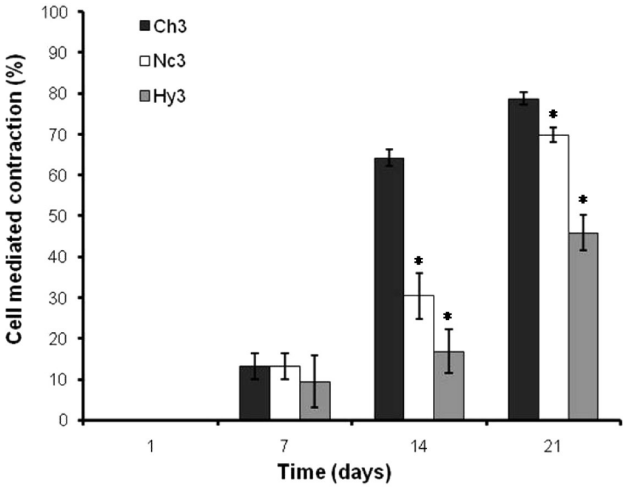

Figure 7. Cell-mediated contraction of the collagen hydrogels (Ch3), nanocomposites (Nc3), and hybrids (Hy3) relative to hydrogel diameter at $t = 0$. Results are expressed as mean ± SD from triplicates experiments. * indicates statistical significance ($p < 0.05$) from student test.

and Hy3 but lower for Nc3, an observation that can be related to higher pore size in the pure collagen and hybrid materials that can favor colonization, compared to lower pore dimensions in the composite material.

3D Immobilization of Fibroblasts within Concentrated Silica−Collagen Materials. Since 2D culture studies demonstrated variable but sustained proliferation of surface-seeded fibroblasts, we have studied the fate of cells entrapped within the different hydrogels. When fibroblasts are entrapped within collagen hydrogels, they establish surface contact with the biopolymer network to reach suitable adhesion, proliferate, and then contract and remodel their environment.[39] In a first step, it was important to monitor their metabolic activity using the MTT assay. For all materials, this activity increased gradually within all materials from day 1 to 21 (Figure 6). At day 21, the number of metabolically active fibroblasts increased by a factor of 6 within pure collagen gels Ch3. The most important activity was found in Nc3 nanocomposites at all time points; at day 21, the active fibroblasts represented 8.1 times the initial value. Lower fibroblast activity was observed within Hy3 hybrid materials. Indeed, there was no significant proliferation within the first week of culture and only at day 21 did the active fibroblast population reach twice the initial one.

In parallel, the contraction activity of entrapped cells was quantified by the decrease in the surface of the different hydrogels. Over the first 7 days in culture, Ch3 gels presented 87% of the initial surface with no significant differences with respect to silicified collagen gels. After 7 days, the surface rapidly decreased for Ch3, with 36% of the surface at day 14 and reaches 20% of the initial surface after 21 days. The addition of silica nanoparticles succeeded in limiting gel contraction in the long term, with 70 and 30% of the initial surface for Nc3 at days 14 and 21, respectively. The lowest contraction rate is observed for Hy3, with 83% after 14 days, and finally reaches 54% at day 21 (Figure 7).

A comparison between MTT and contraction data suggest that the lowest contraction observed for Hy3 composite compared to unsilicified Ch3 can be at least partially correlated with a lower metabolic activity of the entrapped cells. In the case of Nc3, the decrease in contraction compared to Ch3 goes in parallel with

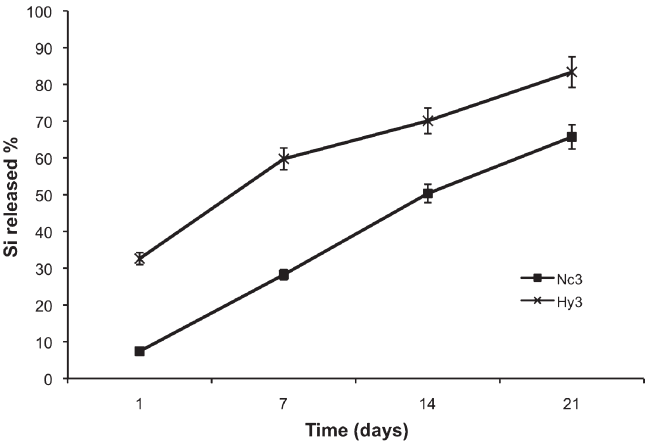

Figure 8. Si released from the nanocomposites (Nc3) and hybrids (Hy3).

an increase in cell metabolic activity. In this context, it was important to check the evolution of the silica content within the materials as porous silica gels and silica particles are prone to dissolve at low concentration in biological media.[40,41] As shown in Figure 8, the release of Si from the composite and hybrid materials, as analyzed by ICP-AES, indicates a faster release from the hybrid Hy3 material, which reaches 83% at the end of the 21 days, compared to composite Nc3, exhibiting 66% dissolution at day 21. An important outcome of this observation is related to the possible toxicity of released Si species. Indeed, it could be speculated that the fast release of 50% Si after 7 days from Hy3 could explain the lowest metabolic activity of fibroblasts at this time point and afterward when compared to Ch3. However, the cell population doubled between day 14 and day 21 when >80% Si had been released. In contrast, cell proliferation in Nc3 was sustained over 21 days of culture despite the fact that 66% nanoparticles was released after this delay. This evidence the absence of toxicity of silica nanoparticles for fibroblasts grown in vitro, in agreement with other reports.[42]

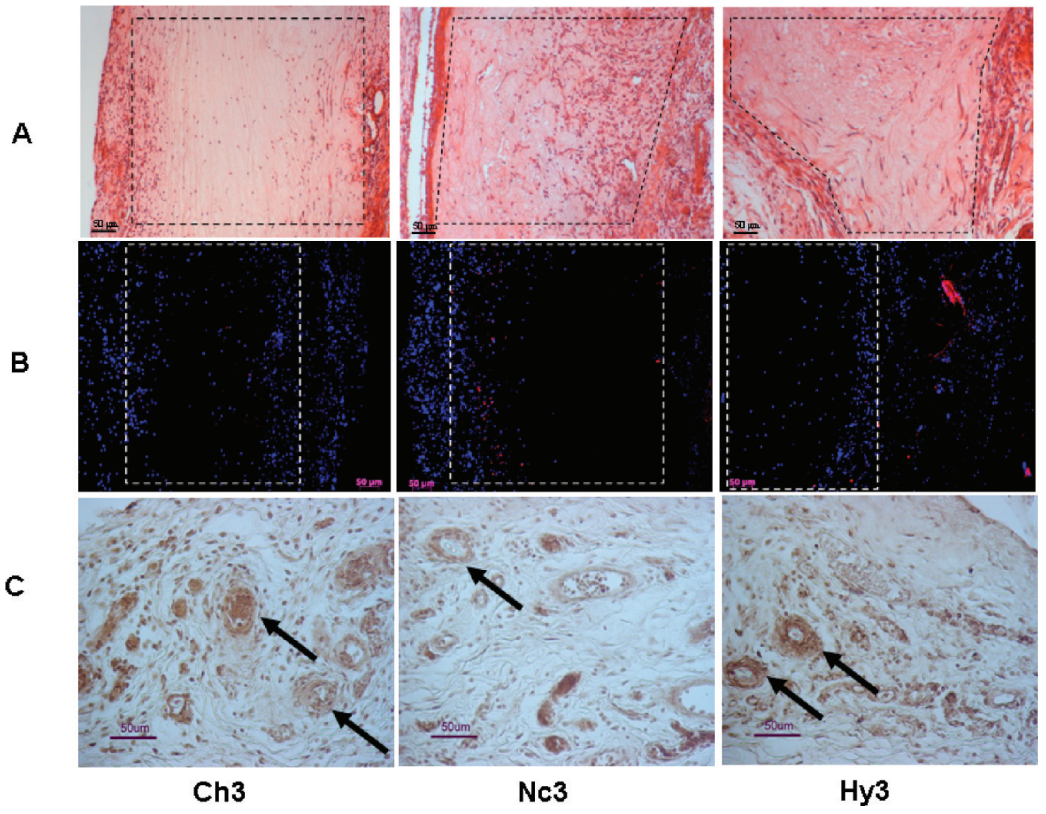

Figure 9. Histological and immunohistological studies 8 days postsurgery. Pure collagen (Ch3), nanocomposite (Nc3), and hybride (Hy3) scaffolds were implanted subcutanously. Sections were stained with hematoxylin-eosin (line A), detection of macrophages (CD68 marker) (line B), and endothelial cells (RECA-1 marker) (line C).

Therefore, the observed variations between Hy3 and Nc3 should be considered in terms of mechanical properties and chemistry/topology of the internal pores that are of considerable importance in 3D environments.[43−46] In this context, it is worth noting a discrepancy between 2D data that indicate better proliferation on Hy3 compared to Nc3 and 3D data. Such a difference has been often reported and attributed to several factors such as cell polarization, absence of nutriments/growth factors gradients and lack of resistance against migration for 2D cultures,[47,48] with strong impact on cellular gene expression, activity, morphology and even differentiation for stem cells.[49] Therefore, some differences between hybrid and composite materials, such as collagen organization, pore geometry but also possible influence of the silica coating on the adhesion and/or nutrients/proteins access to the cells become relevant in 3D.

In vivo Evaluation of Concentrated Silica−Collagen Materials. Since silicification of concentrated collagen gels demonstrated to be an efficient way to improve their mechanical and thermal properties and succeeded in supporting cell viability, adhesion and proliferation to a greater extent, their in vivo integration over the vascular inflammatory phase was investigated (Figure 9). When compared to Ch0 gels, acellular Ch3 hydrogels showed less extensive but significant fibroblast colonization (Figure 9A). Endothelial cells colonization also occurred in all the materials and, similarly to low concentrated collagen gels, organized cells in open tubular structures were observed (Figure 9C). Finally, the infiltration of macrophages was very little in comparison with low concentrated collagen gels, demonstrating that the increase in collagen concentration leads to a moderate inflammatory response (Figure 9B). This difference can be attributed to the fact that materials prepared at low collagen concentration are easily hydrolyzed by metalloproteinases, such as MMP2 (gelatinase), leading to proteolytic fragments that affect multiple functions and properties of inflammatory and immune cell.[50] In fact, the production of MMP2 by fibroblasts was reported to decrease with increasing collagen concentration,[10,28] and thus the production of collagen fragments is also lower, limiting the inflammatory response.

CONCLUSION

The present contribution demonstrates that conditions can be found to obtain collagen-silica homogeneous materials with enhanced thermal and mechanical stability. The composite approach based on the incorporation of preformed colloids appears well-adapted when cellularized materials are targeted due to enhanced preservation of fibroblast activity. Hybrid systems relying of in situ silica formation may be preferred for acellular materials because of a significant increase in thermal and mechanical stability.

In addition, our data indicate that after a 1-week implantation period in subcutaneous sites of rats, no deleterious inflammatory response is observed if sufficient collagen content is used and these materials are colonized by host cells, i.e., fibroblasts and endothelial cells, leading to implant vascularization. Indeed, such an evaluation over the vascular-inflammatory period is only preliminary and in vivo evaluation on the long-term is now necessary to confirm their biocompatibility and establish their

lifetime. An important issue related to the fate of dissolved silica near the implant and its possible access to the systemic circulation is also a major topic of future research. In this context a better control of the dissolution process via chemical and structural modification of the silica network would open the route to the design of drug release materials.

AUTHOR INFORMATION

Corresponding Author

*Fax: +33 144271443. Tel: +33 144271528. E-mail: thibaud.coradin@upmc.fr.

ACKNOWLEDGMENT

M.F.D. thanks the Collège de France for funding and C. Illoul and A. Anglo (LCMCP) for their help with microscopy sample preparation. D. Talbot (PECSA, UPMC-P6) is kindly acknowledged for her collaboration with the ICP-AES measurements. G.J.C. thanks CONICET for funding his travel to Paris.

REFERENCES

(1) de Vos, P.; Bucko, M.; Gemeiner, P.; Navrátil, M.; Svitel, J.; Faas, M.; Strand, B. L.; Skjak-Braek, G.; Morch, Y. A.; Vikartovská, A.; Lacík, I.; Kolláriková, G.; Orive, G.; Poncelet, D.; Pedraz, J. L.; Ansorge-Schumacher, M. B. *Biomaterials* **2009**, *30*, 2559–2570.

(2) Uludag, H.; De Vos, P.; Tresco, P. A. *Adv. Drug Delivery Rev.* **2000**, *42*, 29–64.

(3) Ahlfors, J. E.; Billiar, K. L. *Biomaterials* **2007**, *28*, 2183–91.

(4) Wilkins, L. M.; Watson, S. R.; Prosky, S. J.; Meunier, S. F.; Parenteau, N. L. *Biotechnol. Bioeng.* **1994**, *43*, 747–756.

(5) Raub, C. B.; Putnam, A. J.; Tromberg, B. J.; George, S. C. *Acta Biomater.* **2010**, *6*, 4657–4665.

(6) Bell, E.; Ivarsson, B.; Merrill, C. *Proc. Natl Acad. Sci. U.S.A.* **1979**, *76*, 1274–1278.

(7) Fluck, J.; Querfeld, C.; Cremer, A.; Niland, S.; Krieg, T.; Sollberg, S. *J. Invest. Dermatol.* **1998**, *110*, 153–157.

(8) Hadjipanayi, E.; Mudera, V.; Brown, R. A. *J. Tissue Eng. Regener. Med.* **2009**, *3*, 77–84.

(9) Berry, C. C.; Shelton, J. C.; Lee, D. A. *J. Tissue Eng. Regener. Med.* **2009**, *3*, 43–53.

(10) Helary, C.; Bataille, I.; Abed, A.; Illoul, C.; Anglo, A.; Louedec, L.; Letourneur, D.; Meddahi-Pellé, A.; Giraud-Guille, M. M. *Biomaterials* **2010**, *31*, 481–490.

(11) Wahl, D. A.; Czernuszka, J. T. *Eur. Cell Mater.* **2006**, *11*, 43–56.

(12) Heinemann, S.; Heinemann, C.; Bernhardt, R.; Reinstorf, A.; Nies, B.; Meyer, M.; Worch, H.; Hanke, T. *Acta Biomater.* **2009**, *5*, 1979–1990.

(13) Vallet-Regi, M.; Colilla, M.; Gonzalez, B. *Chem. Soc. Rev.* **2011**, *40*, 596–607.

(14) Marelli, B.; Ghezzi, C. E.; Barralet, J. E.; Boccacini, A. R.; Nazhat, S. N. *Biomacromolecules* **2010**, *11*, 1470–1479.

(15) Desimone, M. F.; Helary, C.; Mosser, G.; Giraud-Guille, M. M.; Livage, J.; Coradin, T. *J. Mater. Chem.* **2010**, *20*, 666–668.

(16) Desimone, M. F.; Helary, C.; Rietveld, I. B.; Bataille, I.; Mosser, G.; Giraud-Guille, M. M.; Livage, J.; Coradin, T. *Acta Biomater.* **2010**, *6*, 3998–4004.

(17) Radin, S.; El-Bassyouni, G.; Vresilovic, E. J.; Schepers, E.; Ducheyne, P. *Biomaterials* **2005**, *26*, 1043–52.

(18) Carturan, G.; Dal Toso, R.; Boninsegna, S.; Dal Monte, R. *J. Mater. Chem.* **2004**, *14*, 2087–2098.

(19) Slowing, I. I.; Vivero-Escoto, J. L.; Wu, C. W.; Lin, V. S. *Adv. Drug Delivery Rev.* **2008**, *60*, 1278–1288.

(20) Hudson, S. P.; Padera, R. F.; Langer, R.; Kohane, D. S. *Biomaterials* **2008**, *29*, 4045–55.

(21) Rosenholm, J. M.; Sahlgren, C.; Linden, M. *Nanoscale* **2010**, *2*, 1870–1883.

(22) Clark, R. A. F.; Ghosh, K.; Tonnesen, M. G. *J. Invest. Dermatol.* **2007**, *127*, 1018–1029.

(23) Bergman, I.; Loxley, R. *Anal. Chem.* **1963**, *35*, 1961–1965.

(24) Mosmann, T. *J. Immun. Methods* **1983**, *65*, 55–63.

(25) Abed, A.; Assoul, N.; Ba, M.; Derkaoui, S. M.; Portes, P.; Louedec, L.; Flaud, P.; Bataille, I.; Letourneur, D.; Meddahi-Pelle, A. *J. Biomed. Mater. Res.* **2011**, *96A*, 535–542.

(26) Brown, R. A.; Phillips, J. B. *Int. Rev. Cytol.* **2007**, *262*, 75–150.

(27) Brown, R. A.; Wiseman, M.; Cho, C. B.; Cheema, U.; Nazhat, S. N. *Adv. Funct. Mater.* **2005**, *15*, 1762–1770.

(28) Hélary, C.; Abed, A.; Mosser, G.; Louedec, L.; Meddahi-Pelle, A.; Giraud-Guille, M. M. *J. Tissue Eng. Regener. Med.* **2011**, *5*, 248–252.

(29) Eglin, D.; Mosser, G.; Giraud-Guille, M. M.; Livage, J.; Coradin, T. *Soft Matter* **2005**, *1*, 129–131.

(30) Eglin, D.; Shafran, K. L.; Livage, J.; Coradin, T.; Perry, C. C. *J. Mater. Chem.* **2006**, *16*, 4220–4230.

(31) Yano, S.; Iwata, K.; Kurita, K. *Mater. Sci. Engin. C* **1998**, *6*, 75–90.

(32) Brasack, I.; Böttcher, H.; Hempel, U. *J. Sol—Gel Sci. Technol.* **2000**, *19*, 479–482.

(33) Ge, Z.; Zhou, Y.; Tong, Z.; Liu, S. *Langmuir* **2011**, *27*, 1143–1151.

(34) Wintgens, V.; Amiel, C. *Macromol. Chem. Phys.* **2008**, *209*, 1553–1563.

(35) Avnir, D.; Coradin, T.; Lev, O.; Livage, J. *J. Mater. Chem.* **2006**, *16*, 1013–1030.

(36) Pelham, R. J.; Wang, Y.-L. *Proc. Natl Acad. Sci. U.S.A.* **1997**, *94*, 13661–13665.

(37) Spiteri, C. G.; Pillar, R. M.; Kandel, R. A. *J Biomed. Mater. Res., A* **2006**, *78*, 676–683.

(38) Anselme, K.; Ploux, L.; Ponche, A. *J. Adhes. Sci Technol.* **2010**, *24*, 831–852.

(39) Feng, Z.; Yamato, M.; Akutsu, T.; Nakamura, T.; Okano, T.; Umezu, M. *Artif. Organs* **2003**, *27*, 84–91.

(40) Finnie, K. S.; Waller, D. J.; Perret, F. L.; Krause-Heuer, A. M.; Lin, H. Q.; Hanna, J. V.; Barbé, C. J. *J. Sol—-Gel Sci. Technol.* **2009**, *49*, 12–18.

(41) Bass, J. D.; Grosso, D.; Boissière, C.; Belamie, E.; Coradin, T.; Sanchez, C. *Chem. Mater.* **2007**, *19*, 4349–4356.

(42) Zhang, Y.; Hu, L.; Yu, D.; Gao, C. *Biomaterials* **2010**, *31*, 8465–8474.

(43) Gardel, M.; Ulrich, S. *J. Phys.: Condens. Matter* **2010**, *22*, 190301and references therein.

(44) Place, E. S.; Evans, D.; Stevens, M. M. *Nat. Mater.* **2009**, *8*, 457–470.

(45) Hale, N. A.; Yang, Y.; Rajagopalan, P. *ACS Appl. Mater. Interface* **2010**, *2*, 2317–2324.

(46) Winer, J. P.; Oake, S.; Janmey, P. A. *PLoS ONE* **2009**, *4*, e6382.

(47) Tibbit, M. W.; Anseth, K. S. *Biotechnol. Bioeng.* **2009**, *103*, 655–663.

(48) Barralet, J. E.; Wang, L.; Lawson, M.; Triffitt, J. T.; Cooper, P. R.; Shelton, R. M. *J. Mater. Sci.: Mater. Med.* **2005**, *16*, 515–519.

(49) Discher, D. E.; Mooney, D. J.; Zandstra, P. W. *Science* **2009**, *324*, 1673–1677.

(50) Adair-Kirk, T. L.; Senior, R. M. *Int. J. Biochem. Cell Biol.* **2008**, *40*, 1101–1110.